ORIGINAL RESEARCH

Postexposure Liponucleotide Prophylaxis and Treatment Attenuates Acute Respiratory Distress Syndrome in Influenza-infected Mice

Lucia E. Rosas[1]*, Lauren M. Doolittle[1]*, Lisa M. Joseph[1], Hasan El-Musa[1], Michael V. Novotny[2], Judy M. Hickman-Davis[3], R. Duncan Hite[4], and Ian C. Davis[1]

[1]Department of Veterinary Biosciences and [3]Department of Veterinary Preventive Medicine, The Ohio State University, Columbus, Ohio; [2]Department of Immunology and Inflammation, Cleveland Clinic, Cleveland, Ohio; and [4]Division of Pulmonary, Critical Care, and Sleep Medicine, Department of Internal Medicine, University of Cincinnati, Cincinnati, Ohio

Abstract

There is an urgent need for new drugs for patients with acute respiratory distress syndrome (ARDS), including those with coronavirus disease (COVID-19). ARDS in influenza-infected mice is associated with reduced concentrations of liponucleotides (essential precursors for *de novo* phospholipid synthesis) in alveolar type II (ATII) epithelial cells. Because surfactant phospholipid synthesis is a primary function of ATII cells, we hypothesized that disrupting this process could contribute significantly to the pathogenesis of influenza-induced ARDS. The goal of this study was to determine whether parenteral liponucleotide supplementation can attenuate ARDS. C57BL/6 mice inoculated intranasally with 10,000 plaque-forming units/mouse of H1N1 influenza A/WSN/33 virus were treated with CDP (cytidine 5'-diphospho)-choline (100 μg/mouse i.p.) ± CDP -diacylglycerol 16:0/16:0 (10 μg/mouse i.p.) once daily from 1 to 5 days after inoculation (to model postexposure influenza prophylaxis) or as a single dose on Day 5 (to model treatment of patients with ongoing influenza-induced ARDS). Daily postexposure prophylaxis with CDP-choline attenuated influenza-induced hypoxemia, pulmonary edema, alterations in lung mechanics, impairment of alveolar fluid clearance, and pulmonary inflammation without altering viral replication. These effects were not recapitulated by the daily administration of CTP (cytidine triphosphate) and/or choline. Daily coadministration of CDP-diacylglycerol significantly enhanced the beneficial effects of CDP-choline and also modified the ATII cell lipidome, reversing the infection-induced decrease in phosphatidylcholine and increasing concentrations of most other lipid classes in ATII cells. Single-dose treatment with both liponucleotides at 5 days after inoculation also attenuated hypoxemia, altered lung mechanics, and inflammation. Overall, our data show that liponucleotides act rapidly to reduce disease severity in mice with severe influenza-induced ARDS.

Keywords: alveolar type II cell; influenza; phospholipid; liponucleotide; surfactant

Clinical Relevance

We showed previously the influenza A virus infection inhibits production of liponucleotides, which are rate-limiting intermediates in *de novo* phospholipid synthesis. Here, we show that postexposure prophylaxis and treatment of influenza A virus–infected mice with liponucleotides attenuate influenza-induced acute respiratory distress syndrome. Liponucleotides therefore have significant potential for influenza postexposure prophylaxis in high-risk individuals and healthcare workers and for treatment of patients with influenza A (and possibly severe acute respiratory syndrome coronavirus 2 [SARS-CoV-2])–induced acute respiratory distress syndrome.

(Received in original form October 14, 2020; accepted in final form February 18, 2021)

*These authors contributed equally to this study.

Supported by The National Heart, Lung, and Blood Institute at the National Institutes of Health (R01 HL137090) (I.C.D.).

Author Contributions: L.E.R., L.M.D., L.M.J., H.E.-M., M.V.N., J.M.H.-D., and R.D.H. performed experiments, collected and analyzed data, and reviewed and edited the draft manuscript. I.C.D. planned studies, analyzed data, and drafted the manuscript.

Correspondence and requests for reprints should be addressed to Ian C. Davis, D.V.M., Ph.D., The Ohio State University, 307 Goss Lab, 1925 Coffey Road, Columbus, OH 43210. E-mail: davis.2448@osu.edu.

This article has a related editorial.

This article has a data supplement, which is accessible from this issue's table of contents at www.atsjournals.org.

Am J Respir Cell Mol Biol Vol 64, No 6, pp 677–686, June 2021

Originally Published in Press as DOI: 10.1165/rcmb.2020-0465OC on February 19, 2021
Internet address: www.atsjournals.org

Before 2020, there were ~150,000 cases of acute respiratory distress syndrome (ARDS) in the United States each year. However, this number has increased significantly because of the ongoing and expanding coronavirus disease (COVID-19) pandemic, as most deaths are secondary to ARDS (1, 2). Currently, there are no viable ARDS- or COVID-19–specific therapeutics. The potential for ICU overload remains high, and there is an urgent need for new drugs to reduce morbidity and mortality in both patients with COVID-19 and those with other forms of ARDS, particularly with the imminent onset of the upcoming 2021 influenza season.

We showed that the development of severe ARDS in mice infected with H1N1 influenza A virus (IAV), which occurs within 6 days post inoculation (d.p.i.), resulted in alveolar type II (ATII) epithelial cell dysfunction and altered phospholipid metabolism (3–6). Moreover, the liponucleotide (LPN) cytidine 5′-diphosphocholine (CDP-CHO), which is an essential precursor for *de novo* phosphatidylcholine synthesis (7, 8), was undetectable in ATII cells from IAV-infected mice (6). These data indicated that IAV inhibits *de novo* phospholipid synthesis via the CDP-choline (Kennedy) pathway in ATII cells. Because surfactant phospholipid synthesis is a primary function of ATII cells (9), we reasoned that disrupting this process could contribute significantly to the pathogenesis of IAV-induced ARDS. Furthermore, we hypothesized that correcting defective phospholipid synthesis by parenteral LPN supplementation would attenuate IAV-induced ARDS.

We tested this hypothesis by administering LPNs alone or in combination to IAV-infected mice under two distinct treatment regimens. First, to model postexposure prophylaxis (PEP) of persons exposed to an IAV-infected individual, we administered LPNs daily from 1–5 d.p.i. by intraperitoneal injection or oral gavage. Second, to model treatment of patients with ongoing ARDS due to influenza, we administered a single LPN dose by intraperitoneal injection at 5 d.p.i. We found that PEP with CDP-CHO decreased IAV-induced hypoxemia, pulmonary edema, and lung dysfunction without altering viral replication. The LPN CDP-diacylglycerol (16:0/16:0) (CDP-DAG) enhanced the effects of CDP-CHO and completely prevented IAV-induced hypoxemia in mice. In addition, lipidomic analysis of isolated ATII cells showed that daily administration of both LPNs together reversed the influenza-induced reduction in total phosphatidylcholine (PC) and ceramide concentrations and significantly increased concentrations of phosphatidylinositols, lysophospholipids, free fatty acids, and other lipids in ATII cells. Interestingly, however, LPN PEP did not reverse infection-induced decreases in major surfactant phospholipids in ATII cells. Importantly, single-dose treatment with a combination of CDP-CHO and CDP-DAG at 5 d.p.i. was almost as effective as daily administration of CDP-CHO on its own. Finally, both LPN PEP and treatment had profound antiinflammatory effects on the lungs of IAV-infected mice.

On the basis of these findings, and because CDP-CHO is known to be very safe in humans (10), we propose that LPNs may be promising new prophylactic and therapeutic candidates for influenza as well as other forms of viral lung injury and ARDS.

Methods

Approvals

All animal experiments complied with the National Research Council *Guide for the Care and Use of Laboratory Animals* and were approved by The Ohio State University's institutional animal care and use committee. For ethical reasons, we did not perform mortality studies.

Mouse Inoculation

As in our other studies, C57BL/6 mice (Charles River Laboratories) were inoculated intranasally with 10,000 plaque-forming units (pfu) of influenza A/WSN/33 (H1N1) virus in 50 μl PBS with 0.1% BSA under ketamine/xylazine anesthesia (5, 11). Control mice were inoculated with 50 μl virus diluent. Mice were individually marked and weighed every 2 days. Carotid arterial oxygen saturation (Sa_{O_2}) and heart rate were measured every other day using the MouseOx system with a collar clip sensor (Starr Life Sciences Corp.). Data for each experimental group were derived from at least two independent inoculations.

Treatments

Mice were treated by intraperitoneal injection daily (1 to 5 d.p.i.) or at 5 d.p.i. only with sterile 0.9% saline (50 μl/mouse i.p.), 100 μg/mouse choline and/or 100 μg/mouse CTP (cytidine triphosphate) (both Millipore Sigma), or 100 μg/mouse CDP-CHO (Millipore Sigma) ± 10 μg/mouse CDP-DAG (Avanti Polar Lipids), all in 50 μl sterile 0.9% saline. Additional mice were treated daily from 1 to 5 d.p.i. with 100 μg/mouse CDP-CHO + 10 μg/mouse CDP-DAG by oral gavage.

Measurement of BAL Fluid Surface Tension

Cell-free BAL fluid (BALF) was centrifuged at 40,000 × *g* to generate large aggregate surfactant pellets. Final surfactant pellets from three mice per sample were pooled and resuspended in 50 μl saline. The surface tension–lowering activity of the large aggregate surfactant fraction (1.0 mg/ml phospholipid) was measured using a pulsating bubble surfactometer (General Transco) as previously described (12).

ATII Cell Isolation

ATII cells were isolated at 6 d.p.i. from killed mice by a standard lung digestion protocol with negative selection for non-ATII cells (5). Cells were pelleted and stored at −80°C for lipidomic analysis.

Lipidomics

Lipidomic analysis of murine ATII cells was performed by Metabolon. Briefly, ATII cell pellets were homogenized in deionized water and subjected to a modified Bligh-Dyer extraction using methanol/water/dichloromethane in the presence of internal standards. Extracts were dried under nitrogen and reconstituted in a dichloromethane: methanol solution containing ammonium acetate for infusion–mass spectrometry analysis in both positive and negative modes. Individual lipid species were quantified by taking the ratio of the signal intensity of each target compound to that of its assigned internal standard and then multiplying by the concentration of internal standard added to the sample. Lipid class concentrations were calculated from the sum of all molecular species within a class, and fatty acid compositions were determined by calculating the proportion of each class comprised by individual fatty

acids. Data were normalized to sample lysate DNA concentration for statistical analysis.

Statistical Analyses

Descriptive statistics were calculated using Instat software (GraphPad) as previously described (3, 13, 14). Heat maps were generated using free online software (heatmapper.ca) (15). $P < 0.05$ was considered statistically significant.

Other Methods

Additional methods and methodological details are described in a data supplement.

Results

PEP of IAV-infected Mice with LPNs Attenuates Hypoxemia, Bradycardia, and Pulmonary Edema without Affecting Viral Replication

Adult C57BL/6 mice infected with an acutely lethal dose of IAV developed severe hypoxemia (Figure 1A) and bradycardia (Figure 1B) by 4 d.p.i., which progressively worsened over the next 2 days. As early as 4 d.p.i., daily administration of 100 μg/mouse CDP-CHO significantly attenuated hypoxemia, bradycardia, pulmonary edema (Figure 1C), and BALF protein (Figure 1D). With the exception of BALF protein concentrations, these effects were enhanced by the coadministration of 10 μg/mouse CDP-DAG, which prevented development of hypoxemia over the course of infection. Interestingly, viral replication (amplitude and kinetics) did not differ between saline- and CDP-CHO–treated mice, but replication was significantly increased at 2 and 4 d.p.i. after the daily administration of CDP-CHO + CDP-DAG (Figure 1E). Finally, daily PEP with CDP-CHO + CDP-DAG by oral gavage (rather than i.p. injection) also significantly improved oxygenation (increasing carotid Sa_{O_2} at 6 d.p.i. from 85.9% ± 1% to 92.9% ± 2.6%; $P < 0.05$; data not shown in Figure 1).

Beneficial Effects of CDP-CHO PEP Are Not Recapitulated by Its Precursors

Daily postinoculation administration of 100 μg/mouse each of the CDP-CHO precursors choline and/or CTP had no impact on either oxygenation (Figure 2A) or lung water content (Figure 2B) at 6 d.p.i.

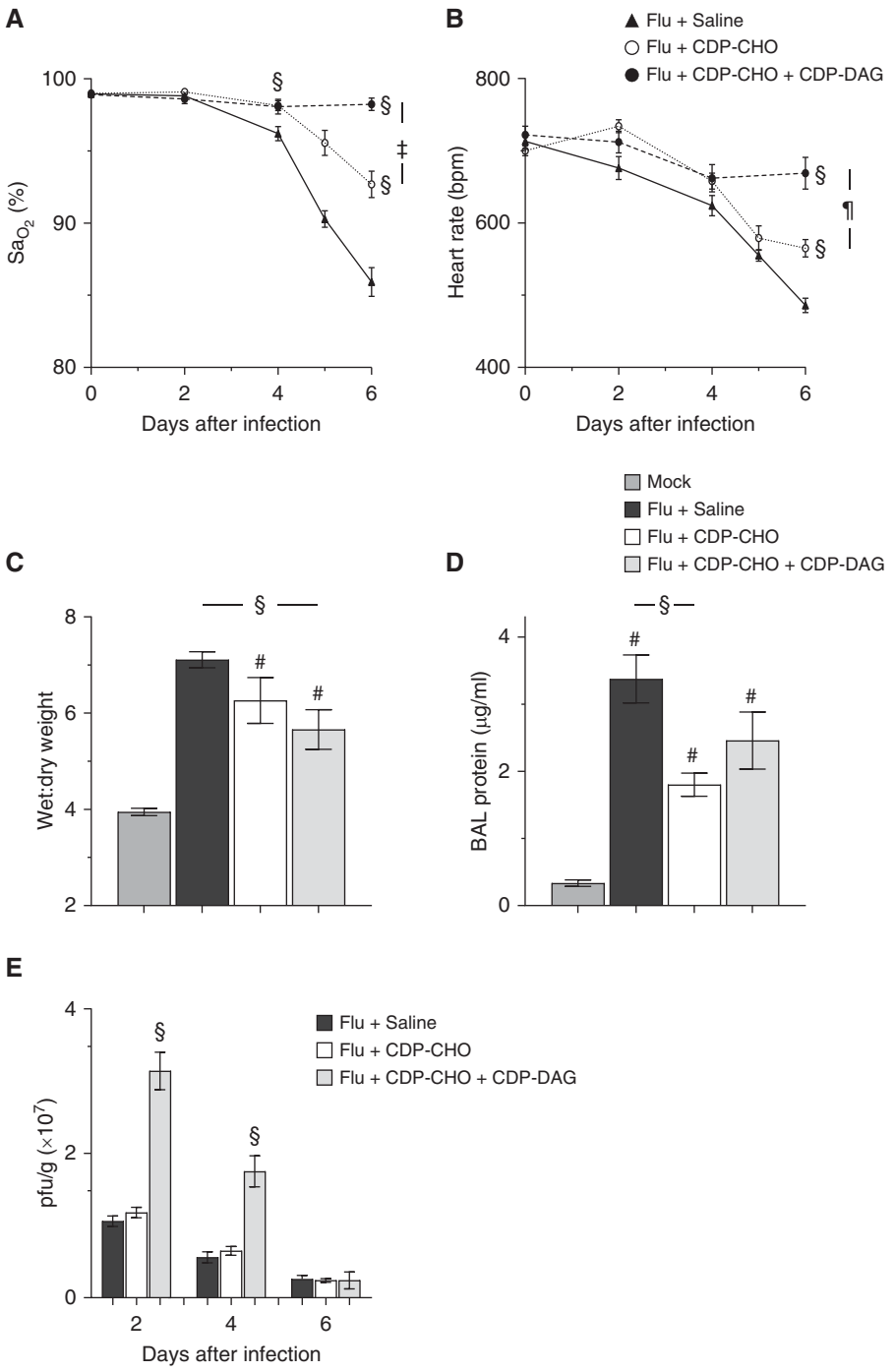

Figure 1. Postexposure prophylaxis (PEP) of influenza A virus (IAV)–infected mice with liponucleotides attenuates hypoxemia, bradycardia, and pulmonary edema without affecting viral replication. Effect of treating C57BL/6 mice infected with H1N1 influenza A/WSN/33 (10,000 plaque-forming units [pfu]/mouse) with sterile 0.9% saline (50 μl/mouse i.p.), 100 μg/mouse cytidine 5′-diphosphocholine (CDP-CHO) (in 50 μl sterile 0.9% saline i.p.), or 100 μg/mouse CDP-CHO + 10 μg/mouse CDP-DAG (in 50 μl sterile 0.9% saline i.p.) daily from 1 to 5 days post inoculation (d.p.i.) on (*A*) carotid Sa_{O_2} (percentage; $n > 10$/group), (*B*) heart rate (beats/min; $n > 10$/group), (*C*) lung water content (wet:dry weight;) at 6 d.p.i. ($n \geq 6$/group), (*D*) BAL fluid protein at 6 d.p.i. (μg/ml; $n = 5$/group), and (*E*) lung homogenate viral titers (pfu × 10^7/g lung tissue; $n = 5$/group). All data were analyzed by ANOVA with a Tukey-Kramer multiple comparison post hoc test and are presented as mean ± SEM. $^{\#}P < 0.001$ versus mock-inoculated mice. $^{\S}P < 0.001$ versus saline-treated, IAV-infected mice. $^{\ddagger}P < 0.005$ and $^{\P}P < 0.001$ versus CDP-CHO–treated, IAV-infected mice. DAG = diacylglycerol; Sa_{O_2} = arterial oxygen saturation.

LPN PEP Improves Lung Function at 6 d.p.i.

IAV infection resulted in a significant increase in basal airway resistance (Figure 3A), accompanied by significant decreases in static lung compliance (Figure 3B) and alveolar fluid clearance rate (Figure 3C). Infection also resulted in a significant increase in BALF minimum surface tension (σ_{min}), indicating impaired surfactant function (Figure 3D). CDP-CHO administration from 1 to 5 d.p.i. restored both static lung compliance and alveolar fluid clearance rate to normal amounts and modestly reduced σ_{min}, although this effect was not statistically significant. Concomitant CDP-DAG administration significantly enhanced CDP-CHO effects on airway resistance but not lung compliance; effects of LPN coadministration on σ_{min} were not measured. Daily LPN administration for 5 days had no effect on cardiovascular function, lung wet:dry weights, lung compliance, or alveolar fluid clearance rate in mock-inoculated mice (*see* Figure E1 in the data supplement).

LPN PEP Attenuates Lung Histopathology at 6 d.p.i.

As in prior studies, lungs from IAV-infected, saline-treated mice showed prominent peribronchial and perivascular mononuclear cell and neutrophil infiltrates together with severe alveolitis and congestion (*see* Figure E2A). Administration of CDP-CHO from 1 to 5 d.p.i. did not significantly attenuate perivascular and peribronchial infiltrates but did reduce the severity of alveolitis (Figure E2B). Concomitant administration of CDP-DAG did not further attenuate lung pathology to any significant degree (Figure E2C).

LPN PEP has Antiinflammatory Effects in IAV-infected Mice

CDP-CHO PEP did not alter BALF macrophage (Figure 4A) and neutrophil (Figure 4B) counts at 5 d.p.i. but decreased them by 60% and 70%, respectively, at 6 d.p.i. PEP with the combination of CDP-CHO + CDP-DAG and had a significantly greater effect on BALF infiltrates at 6 d.p.i., with macrophage and neutrophil counts decreasing by 90% and 87%, respectively.

CDP-CHO administration from 1 to 5 d.p.i. significantly reduced amounts of the

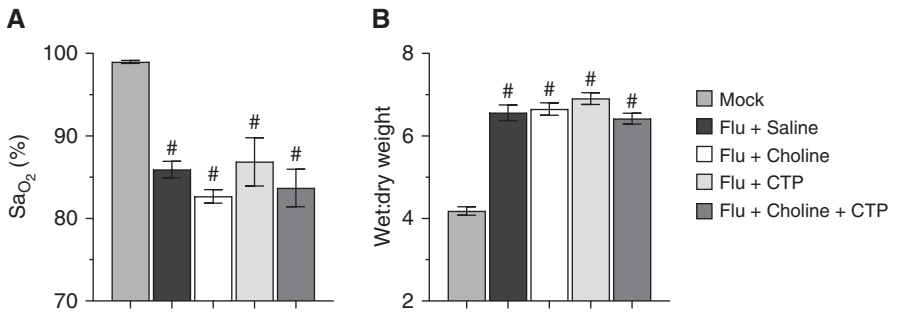

Figure 2. Beneficial effects of CDP-CHO PEP are not recapitulated by its precursors. Effect of treating mice infected with H1N1 influenza A/WSN/33 (10,000 pfu/mouse) with choline, CTP (cytidine triphosphate), or choline + CTP (all 100 μg/mouse, i.p., daily) daily from 1 to 5 d.p.i. on (*A*) carotid Sa_{O_2} (percentage) and (*B*) lung water content (wet:dry weight) at 6 d.p.i. $n \geq 5$/group. All data were analyzed by ANOVA with a Tukey-Kramer multiple comparison post hoc test and are presented as mean ± SEM. $^{\#}P < 0.001$ versus mock-inoculated mice.

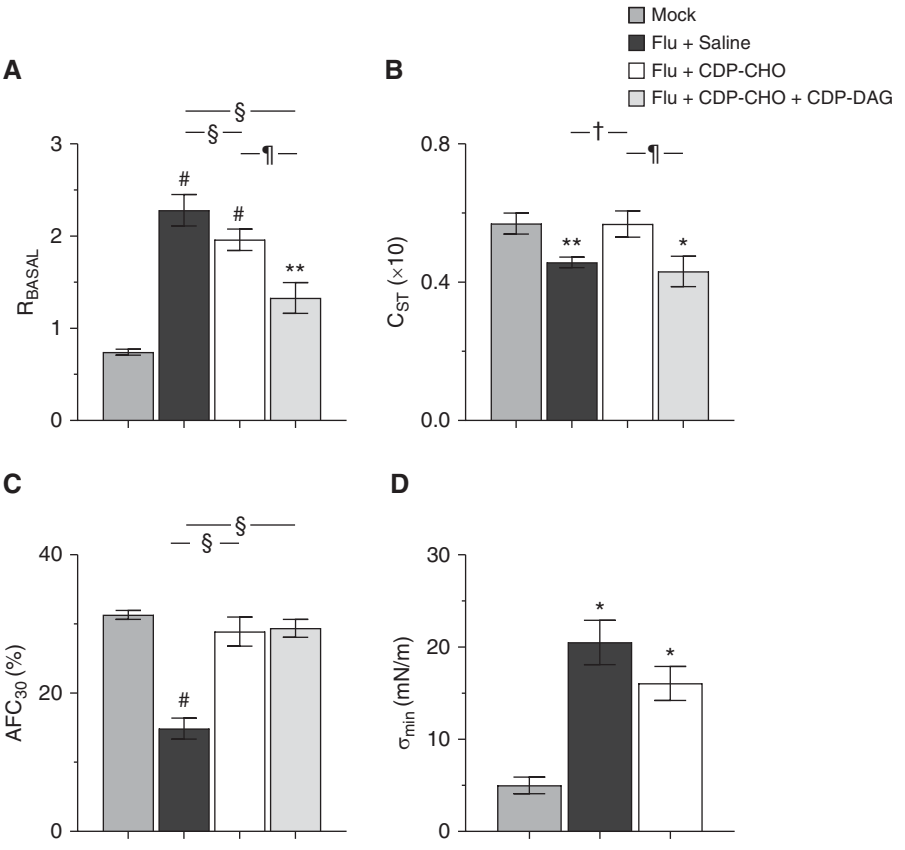

Figure 3. Liponucleotide PEP improves lung function at 6 d.p.i. Effect of treating mice infected with H1N1 influenza A/WSN/33 (10,000 pfu/mouse) with sterile 0.9% saline (50 μl/mouse i.p.), 100 μg/mouse CDP-CHO (in 50 μl sterile 0.9% saline i.p.), or 100 μg/mouse CDP-CHO + 10 μg/mouse CDP-DAG (in 50 μl sterile 0.9% saline i.p.) daily from 1 to 5 d.p.i. on (*A*) R_{BASAL} (cm H_2O.s/ml; $n \geq 6$/group), (*B*) C_{ST} (ml/cm $H_2O \times 10$; $n \geq 6$/group), (*C*) AFC_{30} (percentage; $n \geq 5$/group), and (*D*) BAL fluid σ_{min} achieved over 10 minutes (σ_{min}; mN/m; $n = 2$ samples/group and $n = 3$ mice/sample; flu + CDP-CHO + CDP-DAG group not done). All data were analyzed by ANOVA with a Tukey-Kramer multiple comparison post hoc test and are presented as mean ± SEM. $^{*}P < 0.05$, $^{**}P < 0.005$, and $^{\#}P < 0.001$ versus mock-inoculated mice. $^{\dagger}P < 0.05$ and $^{\S}P < 0.001$ versus saline-treated, IAV-infected mice. $^{\P}P < 0.001$ versus CDP-CHO-treated, IAV-infected mice. σ_{min} = minimal stable surface tension; AFC_{30} = alveolar fluid clearance rate; C_{ST} = static lung compliance; R_{BASAL} = basal airway resistance.

proinflammatory cytokine IFN-γ in BALF at 6 d.p.i. (Figure 4C), and increased BALF IL-6 and IL-10. PEP with CDP-CHO + CDP-DAG had comparable effects on BALF IFN-γ and IL-10 at 6 d.p.i. but caused a significantly greater increase in IL-6 than CDP-CHO alone.

Daily PEP with CDP-CHO did not alter concentrations of the murine neutrophil chemoattractant chemokine KC/CXCL-1 in BALF of IAV-infected mice (Figure 4D). However, BALF from CDP-CHO–treated mice contained much higher concentrations of the MCP-1/CCL-2 (chemokines macrophage chemotactic protein-1) and MIP-1α/CCL-3 (macrophage inflammatory protein-1α). In contrast, PEP with CDP-CHO + CDP-DAG increased BALF KC and MCP-1 but not MIP-1α. Moreover, the effects of CDP-CHO + CDP-DAG administration on MCP-1 were significantly lower than those in mice that received CDP-CHO only from 1 to 5 d.p.i.

PEP with CDP-CHO + CDP-DAG Significantly Modifies the ATII Cell Lipidome

To determine whether beneficial effects of LPN administration result from modulation of the deranged ATII cell lipidome in IAV-infected mice, we performed lipidomic analysis on highly purified ATII cells isolated from mock-inoculated control mice and IAV-infected mice treated daily from 1 to 5 d.p.i. with saline vehicle or CDP-CHO + CDP-DAG. As in our earlier studies, we found significant alterations in the ATII cell lipidome of IAV-infected mice (Figure 5A). In general, concentrations of lipids in each class were consistent across the six mice in the mock-inoculated control group but were much more variable in both IAV-infected, saline-treated and IAV-infected, LPN-treated animals. To overcome this variability and to better define the effects of IAV infection and LPN treatment om the ATII cell lipidome, we evaluated the fold-change in mean values for each lipid category between mock-inoculated mice, IAV-infected, saline-treated mice, and mice receiving daily intraperitoneal injections of CDP-CHO + CDP-DAG from 1 to 5 d.p.i. (Figure 5B). Overall, IAV infection resulted in significant decreases in total PC and ceramide relative to mock-inoculated control animals together with increases in total phosphatidylinositols, free fatty acids, monoacylglycerols, triacylglycerols, and sphingomyelins. However, infection did not alter total phosphatidylethanolamine (PE, which was present in lower amounts than total PC in mock-inoculated mice), lysophospholipids, or diacylglycerols. Total phosphatidylglycerol (PG) was not quantified. Administration of LPNs increased total PC and ceramide almost to control concentrations but decreased lysoPE. Moreover, LPN administration resulted in significant increases in most other lipid classes relative to both mock-inoculated mice and saline-treated, IAV-infected mice. The most dramatic

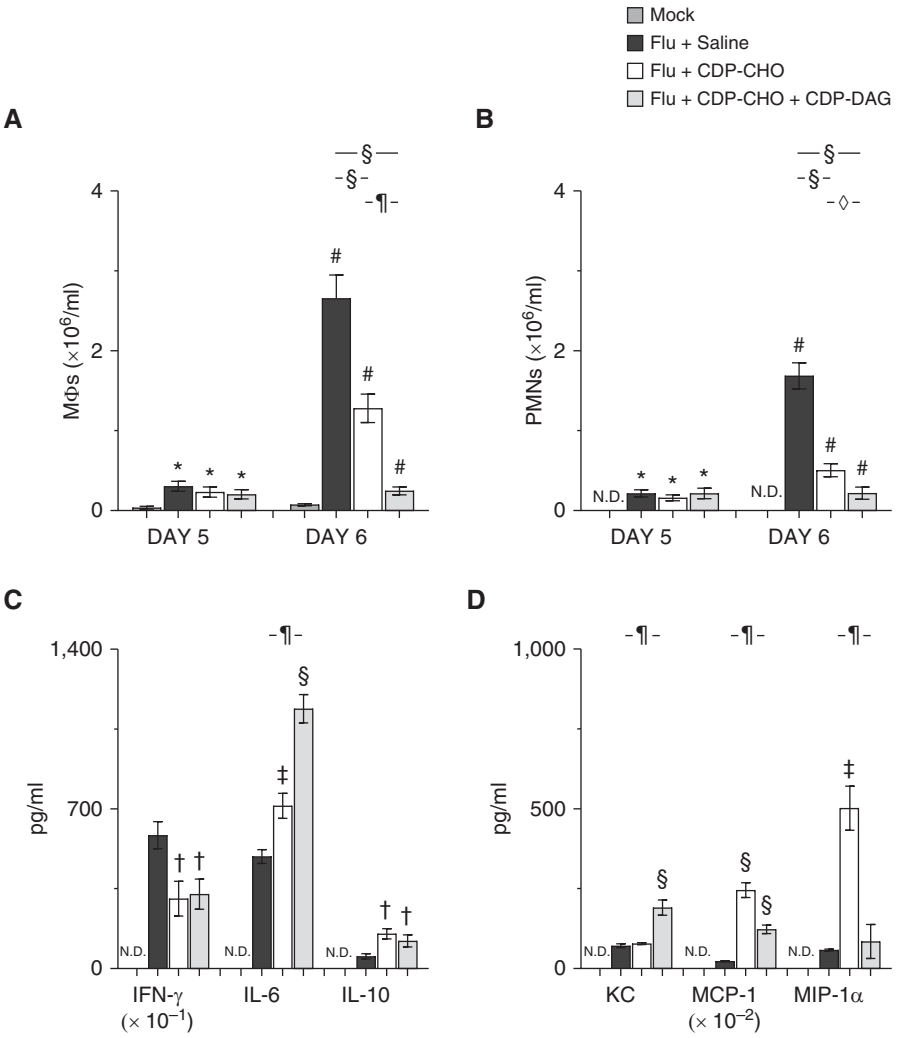

Figure 4. Liponucleotide PEP has antiinflammatory effects in IAV-infected mice. Effect of treating mice infected with H1N1 influenza A/WSN/33 (10,000 pfu/mouse) with sterile 0.9% saline (50 μl/mouse, i.p.), 100 μg/mouse CDP-CHO (in 50 μl sterile 0.9% saline i.p.), or 100 μg/mouse CDP-CHO + 10 μg/mouse CDP-DAG (in 50 μl sterile 0.9% saline i.p.) daily on (*A*) BAL fluid (BALF) MΦs (×10^6/ml; $n \geq 10$/group) at 5 and 6 d.p.i., (*B*) BALF PMNs (×10^6/ml; $n \geq 10$/group) at 5 and 6 d.p.i., (*C*) BALF cytokines (IFN-γ [pg/ml × 10^{-1}], IL-6 [pg/ml], and IL-10 [pg/ml]) ($n \geq 5$/group) at 6 d.p.i., and (*D*) BALF chemokines (KC/CXCL-1 [pg/ml], MCP-1.CCL-2 [macrophage chemotactic protein-1; pg/ml × 10^{-2}], and MIP-1α/CCL-3 [macrophage inflammatory protein-1α; pg/ml]) ($n \geq 5$/group) at 6 d.p.i. All cytokines and chemokines were below the limits of detection in BALF from mock-inoculated mice. All data were analyzed by ANOVA with a Tukey-Kramer multiple comparison post hoc test and are presented as mean ± SEM. $^{*}P < 0.05$ and $^{\#}P < 0.001$ versus mock-inoculated mice. $^{\dagger}P < 0.05$, $^{\ddagger}P < 0.005$, and $^{\S}P < 0.001$ versus saline-treated, IAV-infected mice. $^{\diamond}P < 0.05$ and $^{\P}P < 0.001$ versus CDP-CHO–treated, IAV-infected mice. MΦ = macrophage; MCP-1 = monocyte chemoattractant protein-1; MIP-1α = macrophage inflammatory protein-1α; N.D. = none detected; PMN = neutrophil.

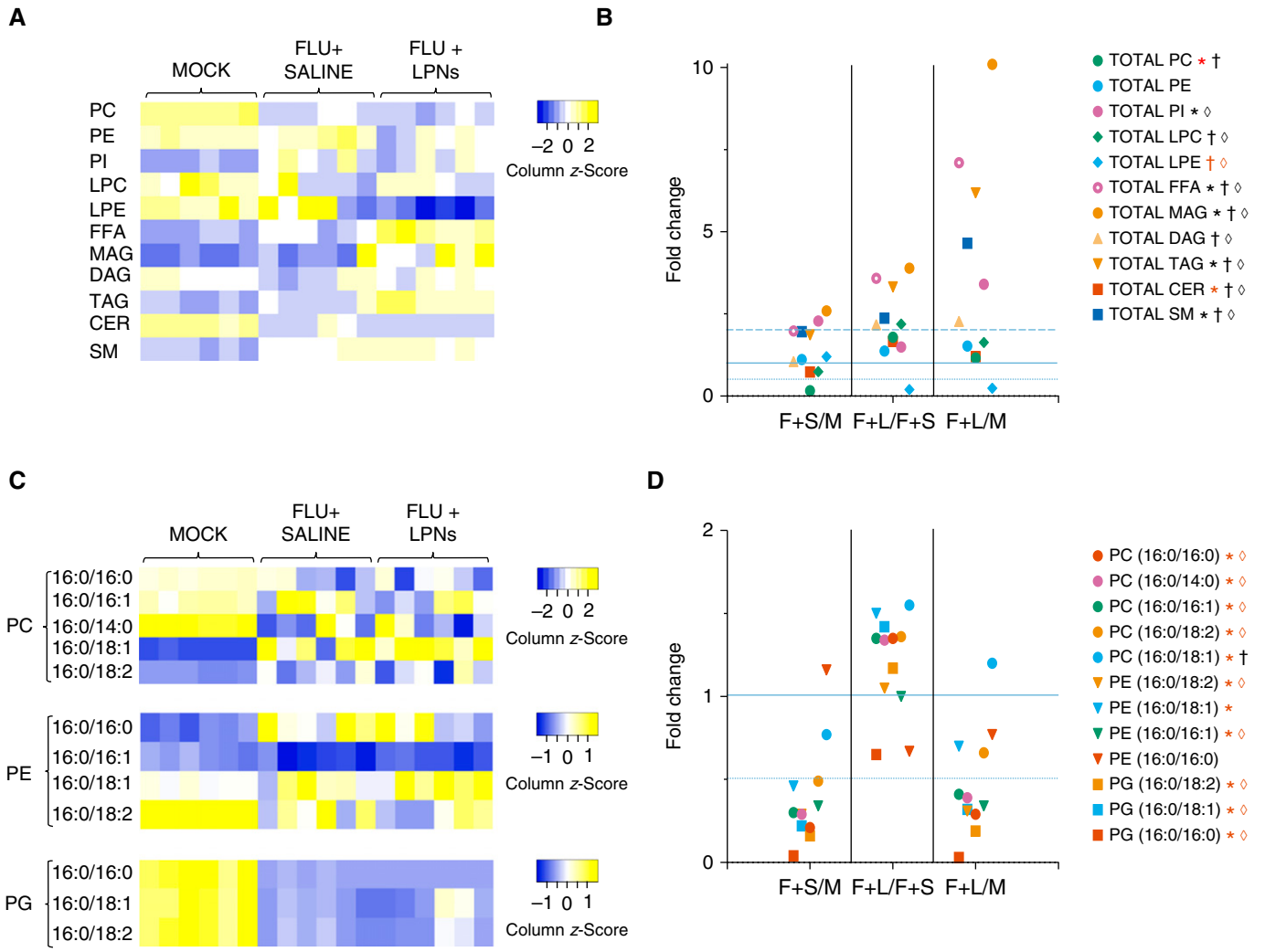

Figure 5. PEP with CDP-CHO + CDP-DAG significantly modifies the alveolar type II (ATII) cell lipidome. Effect of treating mice infected with H1N1 influenza A/WSN/33 (10,000 pfu/mouse) with sterile 0.9% saline (50 μl/mouse i.p.) or 100 μg/mouse CDP-CHO + 10 μg/mouse CDP-DAG (in 50 μl sterile 0.9% saline i.p.) daily from 1 to 5 d.p.i. on (*A*) total amounts of phosphatidylcholine (PC), phosphatidylethanolamine (PE), PI, LPC, LPE, FFA, MAG, DAG, TAG, CER, and SM in ATII cells from individual mice in each treatment group at 6 d.p.i.; (*B*) mean fold-changes in total lipids between ATII cells isolated from mock-inoculated mice (M); IAV-infected, saline-treated mice (F+S); and IAV-infected, LPN-treated mice (F+L) at 6 d.p.i.; (*C*) total amounts of individual surfactant-related palmitoylated PC, PE, and phosphatidylglycerol (PG) species in ATII cells from individual mice in each treatment group at 6 d.p.i.; and (*D*) mean fold-changes in individual surfactant-related palmitoylated PC, PE, and PG species between ATII cells isolated from M, F+S, and F+L. $n = 6$/group. Heatmap colors indicate column *z*-scores (relative to row mean values) from lowest (blue) to highest (yellow). Thin horizontal dotted line indicates fold change = 0.5; solid horizontal line indicates fold change = 1; thick horizontal dotted line indicates fold change = 2. $^{*}P < 0.05$ F+S versus M. $^{\dagger}P < 0.05$ F+L versus F+S. $^{\diamond}P < 0.05$ F+L versus M. Red symbol indicates significant decrease; black symbol indicates significant increase. CER = ceramide; FFA = free fatty acid; LPC = lysophosphatidylcholine; LPE = lysophosphatidylethanolamine; LPN = liponucleotide; MAG = monoacylglycerol; PI = phosphatidylinositol; SM = sphingomyelin; TAG = triacylglycerol.

effects were on monoacylglycerols and triacylglycerols and sphingomyelins.

IAV infection and LPN PEP also significantly modified the surfactant phospholipidome of ATII cells (Figures 5C and 5D). The most abundant PC species in mock-inoculated mice was 16:0/14:0, but ATII cells from these animals also contain significant amounts of PCs 16:0/16:0, 16:0/16:1, 16:0/18.2, 16:0/18:1, and 16:0/18:0 (in descending order of abundance). IAV infection resulted in decreases in all these PC species, and LPN administration only restored PC 16:0/18:1 to normal concentrations. The most abundant PE species was 16:0/18:2, but PEs 16:0/18:1, 16:0/16:1, and 16:0/16:0 were also present in significant amounts. IAV infection decreased all PE species except PE 16:0/16:0, and LPN administration had no significant impact on these effects. Finally, IAV infection also significantly decreased ATII cell PG 16:0/16:0, 16:0/18.1, and 16:0/18.2 (in ascending order of abundance in control cells). LPN administration did not restore PG concentrations to normal.

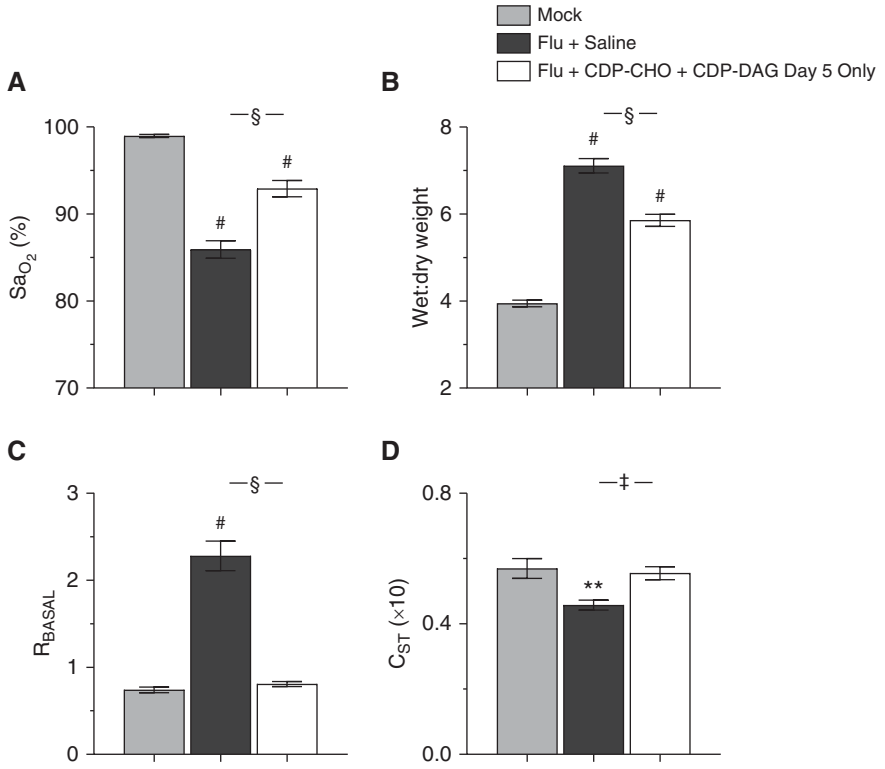

Figure 6. Single-dose LPN treatment improves lung function in mice with severe IAV-induced acute respiratory distress syndrome. Effect of treating mice infected with H1N1 influenza A/WSN/33 (10,000 pfu/mouse) with 100 μg/mouse CDP-CHO + 10 μg/mouse CDP-DAG (both i.p.) at 5 d.p.i. only on 6 d.p.i. values for (*A*) carotid Sa_{O_2} (percentage; $n \geq 14$/group), (*B*) lung water content (wet:dry weight; $n \geq 9$/group), (*C*) R_{BASAL} (cm $H_2O \cdot s$/ml; $n \geq 6$/group), and (*D*) C_{ST} (ml/cm $H_2O \times 10$; $n \geq 6$/group). All data were analyzed by ANOVA with a Tukey-Kramer multiple comparison post hoc test and are presented as mean ± SEM. $^{**}P < 0.005$ and $^{\#}P < 0.001$ versus M at 6 d.p.i. $^{\ddagger}P < 0.005$ and $^{\S}P < 0.001$ versus F+S mice at 6 d.p.i.

Single-Dose LPN Treatment Improves Lung Function in Mice with Severe IAV-induced ARDS

To determine whether LPNs are effective in the face of ongoing lung injury, we treated IAV-infected mice with a single dose of CDP-CHO + CDP-DAG at 5 d.p.i.; we have shown previously that mice exhibit severe ARDS by this time point, and data in the current study confirm that they are severely hypoxemic (*see* Figure 1). Single-dose treatment with both LPNs attenuated hypoxemia (Figure 6A) at 6 d.p.i., reduced lung water content (Figure 6B), normalized basal airway resistance (Figure 6C), and increased static lung compliance to control amounts (Figure 6D). Single-dose LPN treatment at 5 d.p.i. resulted in a modest, but not statistically significant, increase in viral replication at 6 d.p.i. (lung viral titer in LPN-treated mice $0.62 \pm 0.17 \times 10^7$ pfu/g vs. $0.26 \pm 0.11 \times 10^7$ pfu/g in saline-treated mice; data not shown in Figure 6).

Single-Dose LPN Treatment Reduces Pulmonary Inflammation in Mice with Severe IAV-induced ARDS

Treatment with a single dose of CDP-CHO + CDP-DAG at 5 d.p.i. attenuated alveolitis, but to a lesser degree than daily LPN administration (*see* Figure E2D). Single-dose LPN treatment also reduced BALF macrophage and neutrophil counts by 64% and 76%, respectively, at 6 d.p.i. (Figure 7A). Effects of single-dose LPN treatment on BALF cytokines (Figure 7B) and chemokines (Figure 7C) were comparable with those of daily CDP-CHO treatment. In comparison with daily administration of CDP-CHO + CDP-DAG (as shown in Figures 1 and 3), single-dose treatment had significantly less effect on hypoxemia at Day 6 ($P < 0.001$) but had a comparable effect on lung water content and significantly greater effects on airway resistance and lung compliance (both $P < 0.05$).

Discussion

ARDS occurs in 10% of all ICU patients and 23% of those that are mechanically ventilated (16). One-year mortality rates remain high, and many survivors have prolonged and often debilitating lung dysfunction (17). Hence, there is an urgent unmet need for new ARDS treatments. Ideally, these would be inexpensive, stable, safe, and effective irrespective of ARDS etiology.

Using our murine model of IAV-induced ARDS, we showed that PEP (daily postinoculation administration of CDP-CHO) significantly attenuated ARDS severity without altering viral replication. Importantly, combination PEP with both CDP-CHO and CDP-DAG (16:0/16:0) had even greater beneficial effects; when given together daily, they completely prevented development of hypoxemia, attenuated pulmonary edema, and blocked recruitment of leukocytes to the lung at 6 d.p.i. Moreover, even treatment of mice with established severe IAV-induced ARDS with a single dose of this LPN combination was sufficient to attenuate hypoxemia, pulmonary edema, and lung inflammation and to normalize lung function. Importantly, LPNs had no detrimental effects in mock-infected mice. These findings suggested that LPNs may be of value both for preventing development of respiratory failure from influenza in high-risk individuals or healthcare personnel exposed to infected patients (PEP) and for treating patients with established influenza-induced ARDS (treatment).

Our previous studies indicated that IAV infection results in inhibition of CCT-α (phosphocholine cytidylyltransferase-α), which is the enzyme that catalyzes CDP-CHO formation from choline and CTP (18). Importantly, formation of CDP-CHO is the rate-limiting step in *de novo* phosphatidylcholine synthesis. We found that treatment of IAV-infected mice with choline and CTP does not recapitulate the beneficial effects of CDP-CHO, which confirms that CCT-α is not functional in our model. This, in itself, is a surprising finding, as it is generally believed that systemically administered CDP-CHO is rapidly hydrolyzed to CTP and choline by the liver, which are taken up by cells and reconstituted into CDP-CHO before its

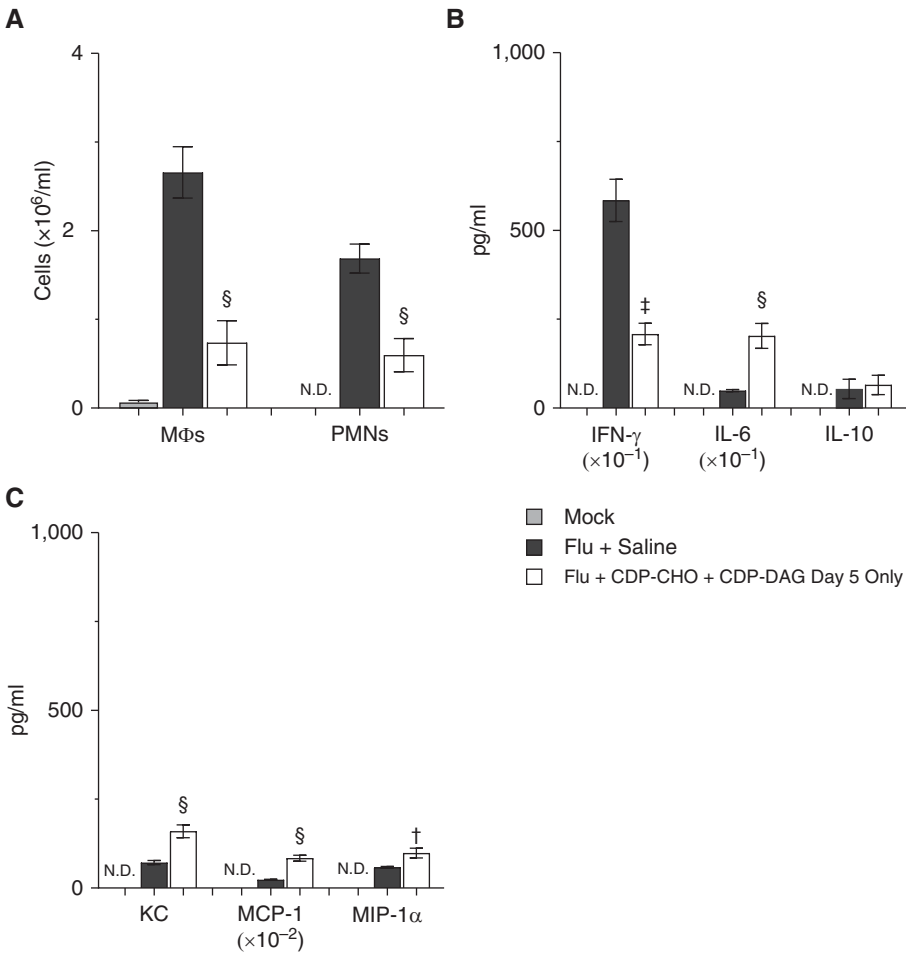

Figure 7. Single-dose LPN treatment reduces pulmonary inflammation in mice with severe IAV-induced acute respiratory distress syndrome. Effect of treating mice infected with H1N1 influenza A/WSN/33 (10,000 pfu/mouse) with 100 μg/mouse CDP-CHO + 10 μg/mouse CDP-DAG (both i.p.) at 5 d.p.i. only on 6 d.p.i. values for (*A*) BALF MΦs ($\times 10^6$/ml; $n \geq 6$/group) and PMNs ($\times 10^6$/ml; $n \geq 6$/group), (*B*) BALF cytokines (IFN-γ [pg/ml $\times 10^{-1}$], IL-6 [pg/ml], and IL-10; [pg/ml]) ($n \geq 5$/group), and (*C*) BALF chemokines (KC/CXCL-1 [pg/ml], MCP-1/CCL-2 [pg/ml $\times 10^{-2}$], and MIP-1α/CCL-3 [pg/ml]) ($n \geq 5$/group). All cytokines and chemokines were below the limits of detection in BALF from M. All data were analyzed by ANOVA with a Tukey-Kramer multiple comparison post hoc test and are presented as mean ± SEM. $^{\dagger}P < 0.05$, $^{\ddagger}P < 0.005$, and $^{\S}P < 0.001$ versus F+S mice at 6 d.p.i.

incorporation into phosphatidylcholine (19).

The mechanisms by which LPNs attenuate hypoxemia, lung dysfunction, and lung injury are not clear. CDP-CHO treatment appears to modestly improve surfactant function in IAV-infected mice, but this effect is unlikely to be clinically significant. It is more likely that the profound antiinflammatory effects of LPNs play a primary role in preventing the onset of severe hypoxemia. Prior studies have shown important roles for both alveolar macrophages and neutrophils in IAV pathogenesis, although how leukocyte infiltration results in development of severe hypoxemia remains unclear (20). Likewise, we do not yet understand why CDP-CHO and CDP-DAG (16:0/16:0) act together so effectively to prevent hypoxemia. CDP-DAG is ineffective in the absence of CDP-CHO (data not shown), but as an important precursor for phosphatidylglycerols, phosphatidylinositols, and the mitochondrial phospholipid cardiolipin, CDP-DAG may broaden the effect of CDP-CHO (21, 22). Alternatively, CDP-DAG (16:0/16:0) could act as a donor of palmitate (16:0) or dipalmitoylated diacylglycerol for *de novo* synthesis of dipalmitoyl-PC by ATII cells. Interestingly, IAV infection resulted in a significant (approximately twofold) increase in free palmitate relative to mock-inoculated control mice, and daily administration of CDP-CHO + CDP-DAG further increased palmitate (by another 3.5-fold; *see* Figure E4). However, it is not yet clear why the administration of both LPNs enhances viral replication at early time points.

PEP with CDP-CHO alone or in combination with CDP-DAG decreased BALF IFN-γ and increased IL-10 to a comparable degree, suggesting the induction of a more antiinflammatory cytokine milieu. Interestingly, CDP-CHO administration dramatically increased BALF IL-6, and this effect was amplified in mice by coadministration of CDP-DAG. In our influenza model, IL-6 appears to play an antiinflammatory role, and the current findings are consistent with that (13, 23). Our data also show that CDP-CHO PEP did not reduce BALF concentrations of the neutrophil chemoattractant KC and dramatically increased BALF macrophage chemoattractant chemokines (MCP-1 and MIP-1α). Moreover, PEP with CDP-CHO + CDP-DAG increased KC and MCP-1 but not MIP-1α. Similar treatment effects were seen in mice that received a single dose of both LPNs at 5 d.p.i., suggesting that some of these differential effects are a consequence of CDP-DAG administration. However, it is not clear how LPNs modulate cytokine production.

Although the effect is quite profound, we also do not know how single-dose LPN treatment of IAV-infected mice at 5 d.p.i. can reduce pulmonary cellular inflammation so rapidly. Our data indicate that at 5 d.p.i., there are no differences in BALF macrophage counts between saline-treated, IAV-infected mice and IAV-infected mice treated with CDP-CHO ± CDP-DAG from 1 to 4 d.p.i., although all are elevated compared with mock-inoculated control mice. This presumably indicates a somewhat modest expansion of the tissue resident macrophage pool over the course of infection (24). However, BALF macrophage counts increase precipitously between 5 and 6 d.p.i. in saline-treated animals. The latter probably reflects the recruitment of proinflammatory monocyte-derived macrophages (25), and it appears to be this effect that is partially or even completely blunted by daily or single-dose LPN administration. However, further

work is necessary to confirm this hypothesis.

The impact of LPN PEP on the ATII cell lipidome was in some ways unexpected. On the basis of our earlier studies (6), we did anticipate that LPNs would reverse the decrease in ATII cell PCs induced by IAV infection, and the current data help to confirm that reduced ATII cell PCs is a consequence of impairment of LPN synthesis by IAV. What was more surprising was the impact of LPN administration on other lipid classes; apart from PEs, LysoPEs, phosphatidylglycerols, and ceramides, all were increased relative to mock-inoculated control animals by LPNs. More interestingly, and despite restoring total PCs to control concentrations, LPN PEP did not normalize any of the most important surfactant PC species in ATII cells; it is possible that this accounts for the limited beneficial effect of LPNs on surfactant function *in vivo*. One caveat to our lipidomic studies is that we did not include an LPN-treated, mock-inoculated control group. Although LPN administration did not significantly alter lung function in mock-inoculated mice, we cannot be sure that it had no effects on the ATII cell lipidome. In that case, differences between mock- and IAV-infected cells might be qualitatively and quantitatively quite different.

LPNs have multiple advantages as influenza therapeutics. They are simple, small, stable, and likely very safe (26) natural metabolites with known antiinflammatory properties (27) that target a highly conserved host metabolic pathway (7). Albeit with varying success, CDP-CHO (as citicoline) has been tested as a therapy for a variety of different diseases of the central nervous system, including acute ischemic stroke (28), vascular cognitive impairment (26), and traumatic brain injury (29), as well as for ischemia/reperfusion-induced cardiac injury (30). There is therefore a large amount of data available describing its pharmacodynamics, pharmacokinetics, and safety in human subjects, and CDP-CHO has excellent bioavailability when administered orally or parenterally (31, 32). Indeed, although effects on hypoxemia were not as dramatic as when administered parenterally, we found that daily LPN administration by oral gavage also resulted in a significant improvement in carotid Sa_{O_2}. An additional advantage of LPNs as influenza therapeutics is that their effects are host directed. The likelihood for development of IAV resistance mutants is therefore far lower than with antiviral drugs such as oseltamivir (33, 34). Moreover, this property means that LPNs may have broader efficacy in ARDS from other causes, including COVID-19. One limitation of our study was that our goal was to show proof of concept, and, consequently, we did not perform comprehensive dose–response and pharmacokinetic studies. Clearly, these will be a necessary component of further drug development.

In conclusion, we demonstrated that daily PEP with CDP-CHO improves oxygenation and lung function and attenuates pulmonary inflammation in mice infected with an acutely lethal dose of IAV. Moreover, we found that CDP-DAG enhances the beneficial effects of CDP-CHO and modulates the ATII cell lipidome without affecting surfactant-related phospholipids. Finally, our data indicate that LPNs can act rapidly to improve oxygenation and reduce pulmonary inflammation even in the presence of ongoing and severe IAV-induced ARDS. On the basis of findings, we propose that LPNs have significant potential both for influenza PEP in high-risk individuals and healthcare workers and for treatment of patients with IAV-induced ARDS. ■

Author disclosures are available with the text of this article at www.atsjournals.org.

Acknowledgment: The authors thank Dr. Andrew Bowman for his assistance in generating influenza A virus stocks.

References

1. Wu C, Chen X, Cai Y, Xia J, Zhou X, Xu S, *et al*. Risk factors associated with acute respiratory distress syndrome and death in patients with coronavirus disease 2019 pneumonia in Wuhan, China. *J Am Med Assoc Intern Med* 2020;180:934–943.
2. Rodriguez-Morales AJ, Cardona-Ospina JA, Gutiérrez-Ocampo E, Villamizar-Peña R, Holguin-Rivera Y, Escalera-Antezana JP, *et al*.; Latin American Network of Coronavirus Disease 2019-COVID-19 Research (LANCOVID-19). Electronic address:https://www.lancovid.org. Clinical, laboratory and imaging features of COVID-19: a systematic review and meta-analysis. *Travel Med Infect Dis* 2020;34:101623.
3. Wolk KE, Lazarowski ER, Traylor ZP, Yu EN, Jewell NA, Durbin RK, *et al*. Influenza A virus inhibits alveolar fluid clearance in BALB/c mice. *Am J Respir Crit Care Med* 2008;178:969–976.
4. Traylor ZP, Aeffner F, Davis IC. Influenza A H1N1 induces declines in alveolar gas exchange in mice consistent with rapid post-infection progression from acute lung injury to ARDS. *Influenza Other Respir Viruses* 2013;7:472–479.
5. Hofer CC, Woods PS, Davis IC. Infection of mice with influenza A/WSN/33 (H1N1) virus alters alveolar type II cell phenotype. *Am J Physiol Lung Cell Mol Physiol* 2015;308:L628–L638.
6. Woods PS, Doolittle LM, Rosas LE, Joseph LM, Calomeni EP, Davis IC. Lethal H1N1 influenza A virus infection alters the murine alveolar type II cell surfactant lipidome. *Am J Physiol Lung Cell Mol Physiol* 2016;311:L1160–L1169.
7. Agassandian M, Mallampalli RK. Surfactant phospholipid metabolism. *Biochim Biophys Acta* 2013;1831:612–625.
8. Goss V, Hunt AN, Postle AD. Regulation of lung surfactant phospholipid synthesis and metabolism. *Biochim Biophys Acta* 2013;1831:448–458.
9. Lopez-Rodriguez E, Gay-Jordi G, Mucci A, Lachmann N, Serrano-Mollar A. Lung surfactant metabolism: early in life, early in disease and target in cell therapy. *Cell Tissue Res* 2017;367:721–735.
10. Adibhatla RM, Hatcher JF. Cytidine 5′-diphosphocholine (CDP-choline) in stroke and other CNS disorders. *Neurochem Res* 2005;30:15–23.
11. Hickman-Davis JM, McNicholas-Bevensee C, Davis IC, Ma HP, Davis GC, Bosworth CA, *et al*. Reactive species mediate inhibition of alveolar type II sodium transport during mycoplasma infection. *Am J Respir Crit Care Med* 2006;173:334–344.
12. Hite RD, Seeds MC, Jacinto RB, Grier BL, Waite BM, Bass DA. Lysophospholipid and fatty acid inhibition of pulmonary surfactant: non-enzymatic models of phospholipase A_2 surfactant hydrolysis. *Biochim Biophys Acta* 2005;1720:14–21.
13. Aeffner F, Bratasz A, Flaño E, Powell KA, Davis IC. Postinfection A77-1726 treatment improves cardiopulmonary function in H1N1 influenza-infected mice. *Am J Respir Cell Mol Biol* 2012;47:543–551.
14. Aeffner F, Abdulrahman B, Hickman-Davis JM, Janssen PM, Amer A, Bedwell DM, *et al*. Heterozygosity for the F508del mutation in the cystic fibrosis transmembrane conductance regulator anion channel attenuates influenza severity. *J Infect Dis* 2013;208:780–789.

15. Babicki S, Arndt D, Marcu A, Liang Y, Grant JR, Maciejewski A, *et al*. Heatmapper: web-enabled heat mapping for all. *Nucleic Acids Res* 2016;44:W147–W153.
16. McNicholas BA, Rooney GM, Laffey JG. Lessons to learn from epidemiologic studies in ARDS. *Curr Opin Crit Care* 2018;24: 41–48.
17. Mart MF, Ware LB. The long-lasting effects of the acute respiratory distress syndrome. *Expert Rev Respir Med* 2020;14: 577–586.
18. Ridsdale R, Tseu I, Wang J, Post M. CTP:phosphocholine cytidylyltransferase α is a cytosolic protein in pulmonary epithelial cells and tissues. *J Biol Chem* 2001;276:49148–49155.
19. Dinsdale JR, Griffiths GK, Rowlands C, Castelló J, Ortiz JA, Maddock J, *et al*. Pharmacokinetics of 14C CDP-choline. *Arzneimittelforschung* 1983;33:1066–1070.
20. Herold S, Becker C, Ridge KM, Budinger GR. Influenza virus-induced lung injury: pathogenesis and implications for treatment. *Eur Respir J* 2015;45:1463–1478.
21. Vance JE. Phospholipid synthesis and transport in mammalian cells. *Traffic* 2015;16:1–18.
22. Schlame M, Greenberg ML. Biosynthesis, remodeling and turnover of mitochondrial cardiolipin. *Biochim Biophys Acta Mol Cell Biol Lipids* 2017;1862:3–7.
23. Woods PS, Tazi MF, Chesarino NM, Amer AO, Davis IC. TGF-β-induced IL-6 prevents development of acute lung injury in influenza A virus-infected F508del CFTR-heterozygous mice. *Am J Physiol Lung Cell Mol Physiol* 2015;308:L1136–L1144.
24. Watanabe S, Alexander M, Misharin AV, Budinger GRS. The role of macrophages in the resolution of inflammation. *J Clin Invest* 2019; 129:2619–2628.
25. Herold S, von Wulffen W, Steinmueller M, Pleschka S, Kuziel WA, Mack M, *et al*. Alveolar epithelial cells direct monocyte transepithelial migration upon influenza virus infection: impact of chemokines and adhesion molecules. *J Immunol* 2006;177:1817–1824.
26. Cotroneo AM, Castagna A, Putignano S, Lacava R, Fantò F, Monteleone F, *et al*. Effectiveness and safety of citicoline in mild vascular cognitive impairment: the IDEALE study. *Clin Interv Aging* 2013;8:131–137.
27. Parrish WR, Rosas-Ballina M, Gallowitsch-Puerta M, Ochani M, Ochani K, Yang LH, *et al*. Modulation of TNF release by choline requires α7 subunit nicotinic acetylcholine receptor-mediated signaling. *Mol Med* 2008;14:567–574.
28. Dávalos A, Alvarez-Sabín J, Castillo J, Díez-Tejedor E, Ferro J, Martínez-Vila E, *et al*.; International Citicoline Trial on acUte Stroke (ICTUS) trial investigators. Citicoline in the treatment of acute ischaemic stroke: an international, randomised, multicentre, placebo-controlled study (ICTUS trial). *Lancet* 2012;380:349–357.
29. Zafonte RD, Bagiella E, Ansel BM, Novack TA, Friedewald WT, Hesdorffer DC, *et al*. Effect of citicoline on functional and cognitive status among patients with traumatic brain injury: citicoline Brain Injury Treatment Trial (COBRIT). *JAMA* 2012;308:1993–2000.
30. Hernández-Esquivel L, Pavón N, Buelna-Chontal M, González-Pacheco H, Belmont J, Chávez E. Citicoline (CDP-choline) protects myocardium from ischemia/reperfusion injury via inhibiting mitochondrial permeability transition. *Life Sci* 2014;96:53–58.
31. Grieb P. Neuroprotective properties of citicoline: facts, doubts and unresolved issues. *CNS Drugs* 2014;28:185–193.
32. EFSA Panel on Dietetic Products, Nutrition and Allergies (NDA). Scientific opinion on the safety of "citicoline" as a novel food ingredient. *EFSA J* 2013;11:3421.
33. Lina B, Boucher C, Osterhaus A, Monto AS, Schutten M, Whitley RJ, *et al*. Five years of monitoring for the emergence of oseltamivir resistance in patients with influenza A infections in the Influenza Resistance Information Study. *Influenza Other Respir Viruses* 2018; 12:267–278.
34. Sato M, Takashita E, Katayose M, Nemoto K, Sakai N, Hashimoto K, *et al*. Detection of variants with reduced baloxavir marboxil susceptibility after treatment of children with influenza A during the 2018-2019 influenza season. *J Infect Dis* 2020;222:121–125.